Available online at www.sciencedirect.com
SCIENCE DIRECT®
International Journal of Solids and Structures 41 (2004) 7129–7153
INTERNATIONAL JOURNAL OF SOLIDS and STRUCTURES
www.elsevier.com/locate/ijsolstr

Change in thickness in curved fold model for axial crushing of tubes

B.L. Tyagi [a], H. Abbas [b,*], M. Arif [b], N.K. Gupta [c]

[a] National Hydroelectric Power Corporation Limited, Faridabad 121 003, India
[b] Department of Civil Engineering, Aligarh Muslim University, Aligarh 202 002, India
[c] Department of Applied Mechanics, Indian Institute of Technology Delhi, New Delhi 110 016, India

Received 10 September 2003; received in revised form 30 May 2004
Available online 3 July 2004

Abstract

A partly inside and partly outside curved fold model with variable straight length and stepped variation in the thickness of tube during folding has been developed in the present paper. The variation of circumferential strain during the formation of fold has been taken into consideration. All model parameters viz. size of fold, optimal value of folding parameter, maximum hinge angle and the final radius of curvature of fold have been evaluated analytically. An expression has been derived for determining the variation of crushing load during the formation of a fold. The total outside and total inside fold models can be easily derived from the present model. The results have been compared with experiments and reasonably good agreement has been observed. The incorporation of change in thickness of tube during folding has been found to reduce the folding parameter thus bringing it closer to the experiments. Some parametric studies by varying the length of straight portion of the fold have also been conducted. The results are of help in understanding the phenomenon of actual fold formation.

Keywords: Axi-symmetric crushing; Energy absorption; Change in thickness; Curved fold model; Outside/inside folding; Cylindrical tubes

1. Introduction

Aircrafts, ships and space vehicles etc. have to withstand an accidental crash for which efficient energy-absorbing devices are required. These energy-absorbing devices may be classified under three different categories on the basis of the principle of (a) extrusion, (b) friction, and (c) material deformation. Cylindrical tubes are the most frequently used devices that absorb energy by material deformation.

Alexander (1960) carried out the pioneering work of analysis of cylindrical tubes under axial crushing in concertina mode considering three circumferential hinges and two straight limbs in between the hinges in

* Corresponding author. Tel.: +91-571-2421521; fax: +91-571-2700528.
E-mail address: abbas_husain@hotmail.com (H. Abbas).

0020-7683/$ - see front matter © 2004 Elsevier Ltd. All rights reserved.
doi:10.1016/j.ijsolstr.2004.05.068

Nomenclature

α	hinge angle
α_m	maximum hinge angle
α_1	an angle
β	ratio of straight length of fold to the half fold length
δ	vertical compression at hinge angle α
δ_T	total effective crushing distance corresponding to one complete fold
f_y	yield strength of material
h	half fold length
k	a parameter
m	folding parameter (= ratio of inside portion of fold to total fold length)
M_p	plastic moment per unit length of tube
P_m	mean crushing load
$\frac{P_m}{P_0}$	non-dimensional mean crushing load
R	initial mean radius of tube
R_A, R_B, R'_B, R'_C	circumferential radii of curvature of tube as shown in Fig. 1
ρ_α	longitudinal radius of curvature at hinge angle α
ρ_f	final radius of curvature of curved portion of fold
t_0	initial thickness of tube
W_b	work done in bending in one complete fold
W_c	work done in circumferential deformation
W_T	total work done in bending and circumferential deformation
W_α	total work done in crushing upto hinge angle α
x	variable curved distance

folding of the tube. In this model, the bending energy was assumed to be localized at the plastic hinges and the circumferential deformation was considered in the straight limbs. He calculated the mean crushing load for which the calculation of only the mean circumferential strain was enough. This model was later extended by Abbas et al. (1989, 1995) to frusta with cylindrical tube considered as a special case by considering total inside folding. Abramowicz and Jones (1984) and Grzebeita (1990) introduced curvature in the deforming fold length. It was found through experiments (Mamalis and Johnson, 1983; Wierzbicki et al., 1992; Gupta and Gupta, 1993; Gupta and Velmurugan, 1997) that folding is partly inside and partly outside the mean diameter of the tube, which was later incorporated in straight fold models (Wierzbicki et al., 1992; Gupta and Abbas, 2000, 2001) as well as the curved fold models (Gupta and Velmurugan, 1997). The variation of crushing load was also estimated in these models for which the variation of circumferential strain during the formation of fold was considered. In the curved fold model of Gupta and Velmurugan (1997), folding parameter, m, which is the ratio of inside to total fold length and the maximum hinge angle was taken either from experiments or it was assumed. In the curved fold model of Grzebeita (1990) and Gupta and Velmurugan (1997), the straight portion of the fold was taken as one-third of fold length, whereas, Abramowicz and Jones (1984) did not consider any straight portion. In a recent paper (Abbas et al., 2003) on curved fold analysis, the authors estimated all of the model parameters analytically instead of assuming them and the straight portion of fold was taken as a variable. The present paper is its extension in which the change in the thickness of tube as considered in an earlier paper of straight fold analysis (Gupta and Abbas, 2000) has been incorporated. All of the model parameters viz. size of fold,

folding parameter, maximum hinge angle and hence the final radius of curvature of hinges have been determined analytically.

Without consideration of the change in thickness, the fold parameter is found to be more than 0.5, whereas, experiments (Gupta and Velmurugan, 1997) show that its value should be less than 0.5. Incorporating the change in thickness in the model, the fold parameter comes closer to experiments. The total outside and the total inside fold models can be easily derived from the present model.

2. Analysis for axial crushing of cylindrical tubes

Considering a cylindrical tube of mean radius, R, and initial thickness t_0 for the purpose of its analysis. The tube is undergoing axi-symmetric axial crushing. Let h be the half fold length out of which mh is inside and $(1-m)\,h$ is outside the mean radius as shown in Fig. 1. In the analysis that follows, it is assumed that the fold formation is symmetrical about its middle-plane and the tube folds both internally and externally. The folding are partly curved and partly straight with the length of straight portion as βh.

The hinge angles corresponding to the hinges at A and C are assumed to be the same. As seen from these figures, the point A′ is the position of the mean radius, R. The portion AA′ folds inside and portion A′C folds outside. The point A′ may lie in curved portion AB or in the straight portion BB′ or in curved portion B′C. The analysis given in this paper depends upon these three cases namely Case I, II and III respectively. All the three cases have been shown in Fig. 1.

As the surface area of the portion of the tube in the process of deformation, there will be change in the thickness of the tube. There will be decrease in thickness in outside portion of the fold due to circumferential stretching and increase in thickness during circumferential compression in its inside portion. In the present paper stepped change in the thickness of tube as considered in an earlier paper on straight fold

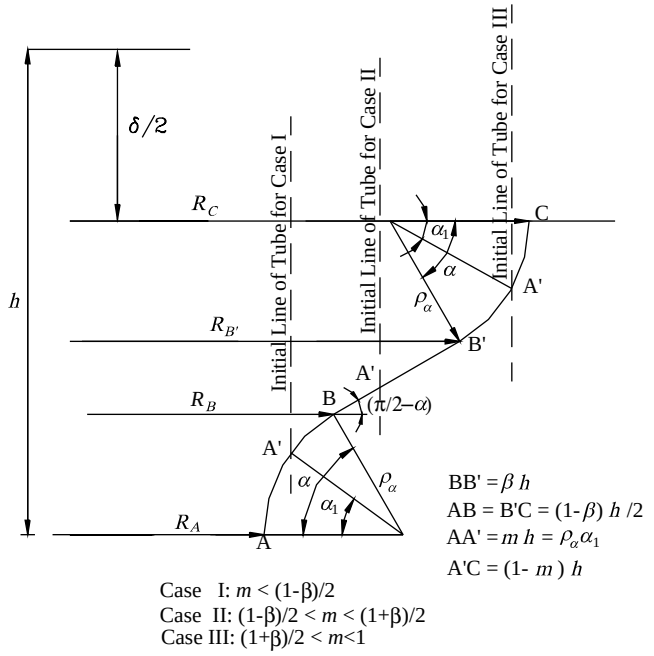

Fig. 1. Folding mechanisms of tube for different cases.

model (Gupta and Abbas, 2000) has been considered. The average thickness of tube in the inside portion of the fold has been taken as t_1, whereas the average thickness of the outside portion has been taken as t_2, as shown in Fig. 2. The values of t_1 and t_2 have been determined by considering no change in volume and hence the change in thickness due to axial stresses has been neglected. The initial volume of inside portion, AA′ and outside portion, A′C of round tube can be calculated as:

$$\text{Volume of inside portion of fold,} \quad V_{01} = 2\pi R t_0 m h \tag{1}$$

$$\text{Volume of outside portion of fold,} \quad V_{02} = 2\pi R t_0 (1-m) h \tag{2}$$

2.1. Case: I Point A′ lies in curved portion AB i.e. $m \leqslant (1-\beta)/2$

The circumferential radii of curvatures of tube at points A, B, B′ and C (Fig. 1) are given by:

$$R_A = R - \rho_\alpha (1 - \cos\alpha_1) \tag{3}$$

$$R_B = R + \rho_\alpha (\cos\alpha_1 - \cos\alpha) \tag{4}$$

$$R_{B'} = R + \rho_\alpha (\cos\alpha_1 - \cos\alpha) + \beta h \sin\alpha \tag{5}$$

$$R_C = R + \rho_\alpha (1 + \cos\alpha_1 - 2\cos\alpha) + \beta h \sin\alpha \tag{6}$$

where, ρ_α is the longitudinal radius of curvature of AB and B′C at hinge angle α and is given by

$$\rho_\alpha = \frac{(1-\beta)h}{2\alpha} = \frac{mh}{\alpha_1} \tag{7}$$

First, the thickness of tube in inside as well as outside portions has been determined and then these values have been used in the computation of internal work done.

2.2. Mean thickness of inside portion of fold, t_1

The circumferential radius, r, of the tube at any point lying in portion AA′ which is at a distance x from point A measured along the length of the fold (Fig. 1) is given by:

$$r = R - \rho_\alpha \{\cos\alpha_2 - \cos\alpha_1\} \tag{8}$$

where $\alpha_2 = \left(\frac{x\alpha_1}{mh}\right)$.

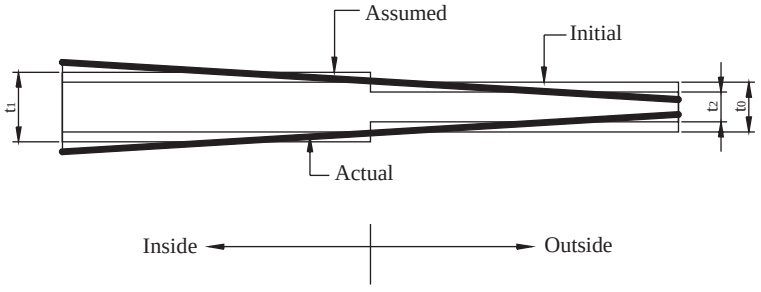

Fig. 2. Variation in thickness of the tube.

The volume of curved portion AA′ can be calculated by integrating the incremental volume of tube as:

$$V_{AA'} = \int_0^{mh} 2\pi t_1 r \, dx = 2\pi t_1 (mh)^2 \left[\frac{R}{mh} - \frac{\sin\alpha_1}{\alpha_1^2} + \frac{\cos\alpha_1}{\alpha_1} \right] \tag{9}$$

By equating this volume in defined state to its initial volume, V_{01} given by Eq. (1), the average thickness of inside portion of the tube can be found from the relation:

$$t_1 = \frac{Rt_0}{mh\left[\frac{R}{mh} + \frac{\cos\alpha_1}{\alpha_1} - \frac{\sin\alpha_1}{\alpha_1^2}\right]} \tag{10}$$

2.3. Mean thickness of outside portion of fold, t_2

The outside portion of the tube consists of three portions viz. two curved portions A′B, B′C and a straight portion BB′ in between. The volume of tube in these portions has been calculated in the following. The sum of these volumes which will be the volume of outside portion of the tube in the deformed state, has been equated to the initial volume to find the average thickness of outside portion of the tube.

The circumferential radius, r, of the tube at any point which is lying in portion A′B at a distance x from point A (i.e. $x > mh$) measured along the length of the fold (Fig. 1) is given by:

$$r = R + \rho_\alpha[\cos\alpha_1 - \cos\alpha_2] \tag{11}$$

The volume of curved portion A′B can be calculated by integrating the incremental volume of tube as:

$$\begin{aligned} V_{A'B} &= \int_{mh}^{(1-\beta)h/2} 2\pi t_2 r \, dx \\ &= 2\pi t_2 \left[R\left\{ \frac{(1-\beta)h}{2} - mh \right\} + mh\left\{ \frac{(1-\beta)h}{2} - mh \right\} \frac{\cos\alpha_1}{\alpha_1} - (mh)^2 \left(\frac{\sin\alpha}{\alpha_1^2} - \frac{\sin\alpha_1}{\alpha_1^2} \right) \right] \end{aligned} \tag{12}$$

The circumferential radius, r, of the tube at any point which is lying in portion BB′ at a distance x measured from point B is given by:

$$r = R + \rho_\alpha(\cos\alpha_1 - \cos\alpha) + x\sin\alpha \tag{13}$$

The volume of straight portion BB′ can be calculated by integrating the incremental volume of tube from the relation:

$$V_{BB'} = \int_0^{\beta h} 2\pi t_2 r \, dx = 2\pi t_2 \beta h \left[R + \frac{mh}{\alpha_1}(\cos\alpha_1 - \cos\alpha) + \frac{\beta h}{2}\sin\alpha \right] \tag{14}$$

The circumferential radius, r, of the tube at any point which is lying in portion B′C at a distance x from point C measured along the length of the fold is given by:

$$r = R + \beta h \sin\alpha + \rho_\alpha[\cos\alpha_1 - 2\cos\alpha + \cos\alpha_2] \tag{15}$$

The volume of curved portion B′C can be calculated by integrating the incremental volume of tube from the relation:

$$V_{B'C} = 2\pi t_2 \int_0^{(1-\beta)h/2} r \, dx = 2\pi t_2 \left[\frac{(1-\beta)h}{2} \left(R + \beta h \sin\alpha + \frac{mh}{\alpha_1}(\cos\alpha_1 - 2\cos\alpha) \right) + \frac{(mh)^2}{\alpha_1^2}\sin\alpha \right] \tag{16}$$

By equating the volume of outside portion in defined state of the tube to its initial volume, V_{02} given by Eq. (2), the average thickness of outside portion of the tube can be found from the relation:

$$t_2 = \frac{2\pi R t_0 (1-m) h}{\left(\frac{V_{A'B}}{t_2} + \frac{V_{BB'}}{t_2} + \frac{V_{B'C}}{t_2}\right)} \tag{17}$$

It is to be noted here that the term t_2 appearing on the right hand side in the denominator gets eliminated when the expressions for $V_{A'B}$, $V_{BB'}$ and $V_{B'C}$ are substituted from Eqs. (12), (14) and (16) respectively.

2.4. Energy absorbed in bending

The energy absorbed in bending when angle α gets incremented by $d\alpha$ is given by:

$$dW_b = 2\pi\left[M_{p1}\left(\frac{\alpha_1}{\alpha}\right)(R_A + R) + M_{p2}\left(1 - \frac{\alpha_1}{\alpha}\right)(R + R_B) + M_{p2}(R_{B'} + R_C)\right]d\alpha$$

Putting the values of R_A, R_B, $R_{B'}$ and R_C from Eqs. (3) to (6), we get

$$\begin{aligned} dW_b = 2\pi\Bigg[&M_{p1}\left(\frac{2R\alpha_1}{\alpha} - \frac{mh}{\alpha} + \frac{mh}{\alpha}\cos\alpha_1\right) - M_{p2}\left(\frac{2R\alpha_1}{\alpha} + \frac{mh}{\alpha}\cos\alpha_1 - \frac{mh}{\alpha}\cos\alpha\right) \\ &+ M_{p2}\left(4R + 2\beta h\sin\alpha + \frac{3mh}{\alpha_1}\cos\alpha_1 - \frac{4mh}{\alpha_1}\cos\alpha + \frac{mh}{\alpha_1}\right)\Bigg]d\alpha \end{aligned} \tag{18}$$

M_{p1} and M_{p2} are the plastic moment capacities of the section of the tube for portion AA′ and A′C respectively. These are given by $M_{p1} = kf_y t_1^2$ and $M_{p2} = kf_y t_2^2$, where the value of k for Von–Mises criterion has been taken as $k = \frac{1}{2\sqrt{3}}$, t_1 and t_2 are the average thickness of the inside and outside portion of the fold.

At the start of the collapse of the tube, the hinge angle α will be zero and radius of curvature will be infinite. As the collapse of the tube progresses, the hinge angle increases and radius of curvature of curved portion of fold reduces till the fold in formation comes in contact with the previously formed fold. The hinge angle at this stage will be the maximum hinge angle α_m. No further deformation is considered and hence contact stresses between the two limbs of consecutive folds are not developed. After reaching this stage, next fold is assumed to begin. Therefore in the present analysis each fold is assumed to form independently i.e. there is no simultaneous formation of folds. Total bending energy can now be computed by integrating this expression from 0 to the maximum hinge angle, α_m, thus

$$\begin{aligned} W_b = 2\pi k f_y\Bigg[&2R\int_0^{\alpha_m}\frac{t_1^2\alpha_1}{\alpha}d\alpha - mh\int_0^{\alpha_m}\frac{t_1^2 d\alpha}{\alpha} + mh\int_0^{\alpha_m} t_1^2\frac{\cos\alpha_1}{\alpha}d\alpha - 2R\int_0^{\alpha_m} t_2^2\frac{\alpha_1}{\alpha}d\alpha \\ &- mh\int_0^{\alpha_m} t_2^2\frac{\cos\alpha_1}{\alpha}d\alpha + mh\int_0^{\alpha_m} t_2^2\frac{\cos\alpha}{\alpha}d\alpha + 4R\int_0^{\alpha_m} t_2^2 d\alpha + 2\beta h\int_0^{\alpha_m} t_2^2\sin\alpha\, d\alpha \\ &+ 3mh\int_0^{\alpha_m} t_2^2\frac{\cos\alpha_1}{\alpha_1}d\alpha - 4mh\int_0^{\alpha_m} t_2^2\frac{\cos\alpha}{\alpha_1}d\alpha + mh\int_0^{\alpha_m}\frac{t_2^2 d\alpha}{\alpha_1}\Bigg] \end{aligned} \tag{19}$$

2.5. Circumferential energy

The circumferential energy for different portions viz. AA′, A′B, BB′ and B′C has been calculated in the following:

The change in the circumferential radius of curvature for the portion between A and A′ due to the progress in the crushing of the tube can be obtained from Eq. (8) as:

$$dr = \frac{1}{\alpha_1^2}[\alpha_1 x\sin\alpha_2 + mh\cos\alpha_2 - mh\alpha_1\sin\alpha_1 - mh\cos\alpha_1]d\alpha_1 \tag{20}$$

The incremental hoop strain for portion AA′ can now be obtained from:

$$|\mathrm{d}\varepsilon_\theta| = \left|\frac{\mathrm{d}r}{r}\right| \tag{21}$$

The incremental hoop energy absorbed in the portion AA′ can be calculated from:

$$\mathrm{d}W_{\mathrm{C1}} = f_{\mathrm{y}}\int_v |\mathrm{d}\varepsilon_\theta|\mathrm{d}v = 2\pi f_{\mathrm{y}}\int_0^{mh} \mathrm{d}r t_1\,\mathrm{d}x \tag{22}$$

Putting the value of dr from Eq. (20), we get

$$\mathrm{d}W_{\mathrm{C1}} = 2\pi f_{\mathrm{y}} t_1 (mh)^2\left[\frac{2\sin\alpha_1}{\alpha_1^3} - \frac{\sin\alpha_1}{\alpha_1} - \frac{2\cos\alpha_1}{\alpha_1^2}\right]\mathrm{d}\alpha_1 \tag{23}$$

Total circumferential energy in the region AA′ can now be found by integrating it from $\alpha = 0$ to $\alpha = \alpha_{\mathrm{m}}$.

$$W_{\mathrm{C1}} = \frac{4\pi f_{\mathrm{y}} m^3 h^2}{(1-\beta)}\left[2\int_0^{\alpha_{\mathrm{m}}} \frac{t_1\sin\alpha_1}{\alpha_1^3}\mathrm{d}\alpha - \int_0^{\alpha_{\mathrm{m}}} \frac{t_1\sin\alpha_1}{\alpha_1}\mathrm{d}\alpha - 2\int_0^{\alpha_{\mathrm{m}}} \frac{t_1\cos\alpha_1}{\alpha_1^2}\mathrm{d}\alpha\right] \tag{24}$$

The incremental circumferential energies dW_{C2}, dW_{C3} and dW_{C4} in the regions A′B, BB′ and B′C respectively and the corresponding total circumferential energies W_{C2}, W_{C3} and W_{C4} can similarly be found and these are given in the following:

$$\begin{aligned}\mathrm{d}W_{\mathrm{C2}} = \frac{4\pi f_{\mathrm{y}} t_2 (mh)^2}{(1-\beta)}\Bigg[&\left(2m - \frac{(1-\beta)}{2}\right)\frac{\cos\alpha_1}{\alpha_1^2} - \frac{(1-\beta)}{2}\frac{t_2\cos\alpha}{\alpha_1^2} \\ &+ \frac{2m}{\alpha_1^3}(\sin\alpha - \sin\alpha_1) - \left(\frac{(1-\beta)}{2} - m\right)\frac{\sin\alpha_1}{\alpha_1}\Bigg]\mathrm{d}\alpha\end{aligned} \tag{25}$$

giving,

$$\begin{aligned}W_{\mathrm{C2}} = \frac{4\pi f_{\mathrm{y}} (mh)^2}{(1-\beta)}\Bigg[&\left\{2m - \frac{(1-\beta)}{2}\right\}\int_0^{\alpha_{\mathrm{m}}} \frac{t_2\cos\alpha_1}{\alpha_1^2}\mathrm{d}\alpha - \frac{(1-\beta)}{2}\int_0^{\alpha_{\mathrm{m}}} \frac{t_2\cos\alpha}{\alpha_1^2}\mathrm{d}\alpha \\ &+ 2m\int_0^{\alpha_{\mathrm{m}}} \frac{t_2}{\alpha_1^3}(\sin\alpha - \sin\alpha_1)\mathrm{d}\alpha - \left\{\frac{(1-\beta)}{2} - m\right\}\int_0^{\alpha_{\mathrm{m}}} \frac{t_2\sin\alpha_1}{\alpha_1}\mathrm{d}\alpha\Bigg]\end{aligned} \tag{26}$$

$$\mathrm{d}W_{\mathrm{C3}} = 2\pi f_{\mathrm{y}} t_2 m\beta h^2\left[\frac{\sin\alpha}{\alpha_1} - \frac{2m}{(1-\beta)}\left(\frac{\sin\alpha_1}{\alpha_1} + \frac{\cos\alpha_1}{\alpha_1^2}\right) + \frac{2m}{(1-\beta)}\frac{\cos\alpha}{\alpha_1^2} + \frac{\beta}{2m}\cos\alpha\right]\mathrm{d}\alpha \tag{27}$$

giving,

$$\begin{aligned}W_{\mathrm{C3}} = 2\pi f_{\mathrm{y}} m\beta h^2\Bigg[&\int_0^{\alpha_{\mathrm{m}}} t_2\frac{\sin\alpha}{\alpha_1}\mathrm{d}\alpha - \frac{2m}{(1-\beta)}\int_0^{\alpha_{\mathrm{m}}} t_2\left(\frac{\sin\alpha_1}{\alpha_1} - \frac{\cos\alpha_1}{\alpha_1^2}\right)\mathrm{d}\alpha \\ &+ \frac{2m}{(1-\beta)}\int_0^{\alpha_{\mathrm{m}}} \frac{t_2\cos\alpha}{\alpha_1^2}\mathrm{d}\alpha + \frac{\beta}{2m}\int_0^{\alpha_{\mathrm{m}}} t_2\cos\alpha\,\mathrm{d}\alpha\Bigg]\end{aligned} \tag{28}$$

$$\begin{aligned}\mathrm{d}W_{\mathrm{C4}} = 2\pi f_{\mathrm{y}} t_2 mh^2\Bigg[&\frac{(1-\beta)}{2}\frac{1}{\alpha_1}\left(2\sin\alpha - \frac{2m}{(1-\beta)}\sin\alpha_1\right) + 3m\frac{\cos\alpha}{\alpha_1^2} - \frac{m}{\alpha_1^2}\cos\alpha_1 \\ &- \frac{4m^2}{(1-\beta)}\frac{\sin\alpha}{\alpha_1^3} + \frac{\beta(1-\beta)}{2m}\cos\alpha\Bigg]\mathrm{d}\alpha\end{aligned} \tag{29}$$

giving,

$$W_{C4} = 2\pi f_y m h^2 \left[\frac{(1-\beta)}{2} \int_0^{\alpha_m} \frac{t_2}{\alpha_1} \left(2\sin\alpha - \frac{2m}{(1-\beta)} \sin\alpha_1 \right) d\alpha + 3m \int_0^{\alpha_m} \frac{t_2 \cos\alpha}{\alpha_1^2} d\alpha \right.$$
$$\left. - \frac{4m^2}{(1-\beta)} \int_0^{\alpha_m} \frac{t_2 \sin\alpha \, d\alpha}{\alpha_1^3} + \frac{\beta(1-\beta)}{2m} \int_0^{\alpha_m} t_2 \cos\alpha \, d\alpha - m \int_0^{\alpha_m} \frac{t_2}{\alpha_1^2} \cos\alpha_1 \, d\alpha \right] \tag{30}$$

2.6. Case II: Point A′ lies in the straight portion BB′ i.e. $\frac{(1-\beta)}{2} < m < \frac{(1+\beta)}{2}$

Similar to Case I, the thickness of tube in inside and outside portions will be determined first and then these values will be used in the computation of internal work done. The circumferential radii of curvatures of tube at points A, B, B′ and C (Fig. 1) are given by:

$$R_A = R - \rho_\alpha(1-\cos\alpha) - \frac{h}{2}(2m+\beta-1)\sin\alpha \tag{31}$$

$$R_B = R - \frac{h}{2}(2m+\beta-1)\sin\alpha \tag{32}$$

$$R_{B'} = R + \frac{h}{2}(1+\beta-2m)\sin\alpha = R_C - \rho_\alpha(1-\cos\alpha) \tag{33}$$

$$R_C = R + \frac{h}{2}(1+\beta-2m)\sin\alpha + \rho_\alpha(1-\cos\alpha) \tag{34}$$

where, ρ_α is the longitudinal radius of curvature of AB and B′C and is given by

$$\rho_\alpha = \frac{(1-\beta)h}{2\alpha} \tag{35}$$

2.7. Mean thickness of inside portion of fold, t_1

The circumferential radius, r, of the tube at any point which is lying in portion AB which is at a distance x from point A measured along the length of the fold (Fig. 1) is given by:

$$r = R + \rho_\alpha[\cos\alpha - \cos\alpha_3] - \frac{h}{2}(2m+\beta-1)\sin\alpha \tag{36}$$

where

$$\alpha_3 = \frac{2x\alpha}{(1-\beta)h}$$

The volume of curved portion AB can be calculated by integrating the incremental volume of tube from the relation:

$$V_{AB} = 2\pi t_1 \int_0^{(1-\beta)h/2} r \, dx$$
$$= \pi(1-\beta)h t_1 \left[R + \frac{(1-\beta)h}{2\alpha}\cos\alpha - \frac{(1-\beta)h}{2\alpha^2}\sin\alpha - \frac{h}{2}(2m+\beta-1)\sin\alpha \right] \tag{37}$$

The circumferential radius, r, of the tube at any point which is lying in portion BA′ at a distance x from point B measured along the length of the fold is given by:

$$r = R - \frac{h}{2}(2m + \beta - 1)\sin\alpha + x\sin\alpha \tag{38}$$

The volume of straight portion BB′ can be calculated by integrating the incremental volume of tube from the relation:

$$V_{BA'} = \int_0^{(2m+\beta-1)h/2} 2\pi r t_1 \,\mathrm{d}x = 2\pi t_1 \frac{h}{2}(2m + \beta - 1)\left[R - \frac{h}{4}(2m + \beta - 1)\sin\alpha\right] \tag{39}$$

By equating the volume of outside portion of the tube in deformed state to its initial volume, V_{01} given by Eq. (1), the average thickness of inside portion of the tube can be found from the relation:

$$t_1 = \frac{2\pi R m h t_0}{\left(\frac{V_{AB}}{t_1} + \frac{V_{BA'}}{t_1}\right)} \tag{40}$$

2.8. Mean thickness of outside portion of fold, t_2

The circumferential radius, r, of the tube at any point which is lying in portion A′B′ at a distance x from point A′ measured along the length of the fold is given by:

$$r = R + x\sin\alpha \tag{41}$$

The volume of straight portion A′B′ can be calculated by integrating the incremental volume of tube from the relation:

$$V_{A'B'} = \int_0^{(\beta-2m+1)h/2} 2\pi r t_2 \,\mathrm{d}x = \pi t_2 h(\beta - 2m + 1)\left[R + \frac{h}{4}(\beta - 2m + 1)\sin\alpha\right] \tag{42}$$

The circumferential radius, r, of the tube at any point which is lying in portion B′C at a distance x from point C measured along the curved length of the fold is given by:

$$r = R + \frac{h}{2}(\beta + 1 - 2m)\sin\alpha + \rho_\alpha(\cos\theta - \cos\alpha) \tag{43}$$

The volume of curved portion B′C can be calculated by integrating the incremental volume of tube from the relation:

$$V_{B'C} = \int_0^{\alpha} 2\pi r t_2 \rho_\alpha \mathrm{d}\theta = 2\pi r t_2 R \frac{(1-\beta)h}{2}\left[R + \frac{h}{2}(\beta + 1 - 2m)\sin\alpha + \frac{(1-\beta)h}{2}\left\{\frac{\sin\alpha}{\alpha^2} - \frac{\cos\alpha}{\alpha}\right\}\right] \tag{44}$$

By equating the volume of outside portion of the tube in deformed state to its initial volume, V_{02}, given by Eq. (2), the average thickness of outside portion of the tube can be found from the relation:

$$t_2 = \frac{2\pi R(1-m)h t_0}{\left(\frac{V_{A'B'}}{t_2} + \frac{V_{B'C}}{t_2}\right)} \tag{45}$$

2.9. Energy absorbed in bending

The incremental energy absorbed in bending is given by

$$\begin{aligned} \mathrm{d}W_{\mathrm{b}} &= 2\pi\lfloor M_{\mathrm{p1}}(R_{\mathrm{A}}+R_{\mathrm{B}})+M_{\mathrm{p2}}(R_{\mathrm{B}'}+R_{\mathrm{C}})\rfloor\mathrm{d}\alpha \\ &= 4\pi M_{\mathrm{p1}}\left[R-\frac{(1-\beta)h}{4\alpha}(1-\cos\alpha)-\frac{h}{2}(2m+\beta-1)\sin\alpha\right]\mathrm{d}\alpha \\ &\quad +4\pi M_{\mathrm{p2}}\left[R+\frac{h}{2}(1+\beta-2m)\sin\alpha+\frac{(1-\beta)h}{4\alpha}(1-\cos\alpha)\right]\mathrm{d}\alpha \end{aligned} \tag{46}$$

Total bending energy can now be computed by integrating this expression from 0 to the maximum hinge angle, α_{m}, thus

$$\begin{aligned} W_{\mathrm{b}} &= 4\pi k f_{\mathrm{y}}\left[R\int_0^{\alpha_{\mathrm{m}}}(t_1^2+t_2^2)\mathrm{d}\alpha-\frac{(1-\beta)h}{4}\int_0^{\alpha_{\mathrm{m}}}\frac{1}{\alpha}(t_1^2-t_2^2)(1-\cos\alpha)\mathrm{d}\alpha\right. \\ &\quad \left.-\frac{h}{2}(2m+\beta-1)\int_0^{\alpha_{\mathrm{m}}}t_1^2\sin\alpha\,\mathrm{d}\alpha+\frac{h}{2}(1+\beta-2m)\int_0^{\alpha_{\mathrm{m}}}t_2^2\sin\alpha\,\mathrm{d}\alpha\right] \end{aligned} \tag{47}$$

2.10. Circumferential energy

The circumferential energy for different portions viz. AB, BA′, A′B′ and B′C has been calculated in the following:

The change in the circumferential radius of curvature for the portion between A and B can be obtained from Eq. (36) as:

$$\mathrm{d}r=\frac{(1-\beta)h}{2\alpha^2}\{\cos\alpha_3-\alpha\sin\alpha-\cos\alpha\}\mathrm{d}\alpha+\frac{x}{\alpha}\sin\alpha_3\,\mathrm{d}\alpha-\frac{h}{2}(2m+\beta-1)\cos\alpha\,\mathrm{d}\alpha \tag{48}$$

The incremental hoop energy absorbed in the portion AB can be calculated as:

$$\begin{aligned} \mathrm{d}W_{\mathrm{C1}} &= \frac{\pi t_1 f_{\mathrm{y}}}{\alpha^2}\int_0^{(1-\beta)h/2}[(1-\beta)h\{\cos\alpha_3-\alpha\sin\alpha-\cos\alpha\}\mathrm{d}\alpha \\ &\quad +2\alpha x\sin\alpha_3\,\mathrm{d}\alpha-\alpha^2 h(2m+\beta-1)\cos\alpha\,\mathrm{d}\alpha\,\mathrm{d}x] \end{aligned}$$

or,

$$\mathrm{d}W_{\mathrm{C1}}=\frac{\pi t_1 f_{\mathrm{y}}(1-\beta)^2h^2}{2\alpha^3}\left[-\alpha^2\sin\alpha-2\alpha\cos\alpha+\sin\alpha-\alpha\cos\alpha+\sin\alpha-\alpha^3\frac{(2m+\beta-1)}{(1-\beta)}\cos\alpha\right]\mathrm{d}\alpha \tag{49}$$

Total circumferential energy in the region AB can now be found by integrating it from $\alpha=0$ to $\alpha=\alpha_{\mathrm{m}}$.

$$\begin{aligned} W_{\mathrm{C1}} &= \pi f_{\mathrm{y}}\frac{(1-\beta)^2h^2}{2}\left[2\int_0^{\alpha_{\mathrm{m}}}\frac{t_1\sin\alpha\,\mathrm{d}\alpha}{\alpha^3}-2\int_0^{\alpha_{\mathrm{m}}}\frac{t_1\cos\alpha}{\alpha^2}\mathrm{d}\alpha-\int_0^{\alpha_{\mathrm{m}}}\frac{t_1\sin\alpha}{\alpha}\mathrm{d}\alpha\right. \\ &\quad \left.-\frac{(2m+\beta-1)}{(1-\beta)}\int_0^{\alpha_{\mathrm{m}}}t_1\cos\alpha\,\mathrm{d}\alpha\right] \end{aligned} \tag{50}$$

The incremental circumferential energy $\mathrm{d}W_{\mathrm{C2}}$, $\mathrm{d}W_{\mathrm{C3}}$ and $\mathrm{d}W_{\mathrm{C4}}$ in the region BA′, A′B′ and B′C respectively and the corresponding total circumferential energy W_{C2}, W_{C3} and W_{C4} can similarly be found and these are given in the following:

$$dW_{C2} = -\pi f_y t_1 \frac{h^2}{4}(2m+\beta-1)^2 \cos\alpha \, d\alpha \tag{51}$$

giving

$$W_{C2} = -\pi f_y \frac{h^2(2m+\beta-1)^2}{4} \int_0^{\alpha_m} t_1 \cos\alpha \, d\alpha \tag{52}$$

$$dW_{C3} = \pi f_y \frac{h^2}{4}(\beta-2m+1)^2 t_2 \cos\alpha \, d\alpha \tag{53}$$

giving

$$W_{C3} = \pi f_y \frac{h^2}{4}(\beta-2m+1)^2 \int_0^{\alpha_m} t_2 \cos\alpha \, d\alpha \tag{54}$$

$$dW_{C4} = \pi f_y t_2 \frac{(1-\beta)^2 h^2}{2}\left[\frac{(\beta+1-2m)}{(1-\beta)}\cos\alpha + \frac{\sin\alpha}{\alpha} + \frac{2\cos\alpha}{\alpha^2} - \frac{2\sin\alpha}{\alpha^3}\right] d\alpha \tag{55}$$

giving

$$W_{C4} = \pi f_y \frac{(1-\beta)^2 h^2}{2}\left[\frac{(\beta+1-2m)}{(1-\beta)}\int_0^{\alpha_m} t_2 \cos\alpha \, d\alpha + \int_0^{\alpha_m} t_2 \frac{\sin\alpha}{\alpha}\left(1-\frac{2}{\alpha^2}\right) d\alpha + 2\int_0^{\alpha_m} \frac{t_2 \cos\alpha}{\alpha^2} d\alpha\right] \tag{56}$$

2.11. Case III: Point A' lies in the curved portion $B'C$ i.e. $\frac{(1+\beta)}{2} < m < 1$

The circumferential radii of curvatures of tube at points A, B, B′ and C (Fig. 1) are given by:

$$R_C = R + \rho_\alpha(1-\cos\alpha_1) \tag{57}$$

$$R_{B'} = R - \rho_\alpha(\cos\alpha_1 - \cos\alpha) \tag{58}$$

$$R_B = R_{B'} - \beta h \sin\alpha = R - \rho_\alpha(\cos\alpha_1 - \cos\alpha) - \beta h \sin\alpha \tag{59}$$

$$R_A = R - \rho_\alpha(\cos\alpha_1 - 2\cos\alpha + 1) - \beta h \sin\alpha \tag{60}$$

where

$$\alpha_1 = \frac{2(1-m)\alpha}{(1-\beta)} \tag{61}$$

and,

$$d\alpha_1 = \frac{2(1-m)}{(1-\beta)} d\alpha \tag{62}$$

2.12. Mean thickness of inside portion of fold, t_1

The circumferential radius, r, of the tube at any point which is lying in portion AB at a distance x from point A measured along the length of the fold is given by:

$$r = R - \rho_\alpha[\cos\alpha_1 - 2\cos\alpha + \cos\alpha_3] - \beta h \sin\alpha \tag{63}$$

The volume of straight portion AB can be calculated by integrating the elemental volume of tube from the relation:

$$V_{AB} = 2\pi t_1 \int_0^{(1-\beta)h/2} r\,dx = \pi t_1 (1-\beta)h\left[R - \beta h \sin\alpha - \frac{(1-\beta)h}{2\alpha}\left\{\cos\alpha_1 - 2\cos\alpha + \frac{\sin\alpha}{\alpha}\right\}\right] \tag{64}$$

The circumferential radius, r, of the tube at any point which is lying in straight portion BB′ at a distance x from point B measured along the length of the fold is given by:

$$r = R - \rho_\alpha(\cos\alpha_1 - \cos\alpha) - \beta h \sin\alpha + x\sin\alpha \tag{65}$$

The volume of straight portion BB′ can be calculated by integrating the elemental volume of tube from the relation:

$$V_{BB'} = 2\pi t_1 \int_0^{\beta h} r\,dx = 2\pi t_1 \beta h\left[R - \frac{(1-\beta)h}{2\alpha}(\cos\alpha_1 - \cos\alpha) - \frac{\beta h}{2}\sin\alpha\right] \tag{66}$$

The circumferential radius, r, of the tube at any point which is lying in portion B′A′ at a distance x from point C measured along the length of the fold is given by:

$$r = R - \rho_\alpha(\cos\alpha_1 - \cos\alpha_3) \tag{67}$$

The volume of curved portion B′A′ can be calculated by integrating the elemental volume of tube from the relation:

$$\begin{aligned} V_{B'A'} &= 2\pi t_1 \int_{(1-m)h}^{(1-\beta)h/2} r\,dx \\ &= \pi h t_1\left[(2m-\beta-1)\left\{R - \frac{(1-\beta)h}{2\alpha}\cos\alpha_1\right\} + (1-\beta)^2\frac{h}{2\alpha^2}(\sin\alpha - \sin\alpha_1)\right] \end{aligned} \tag{68}$$

By equating the volume of inside portion of the tube in deformed state to its initial volume, V_{01}, given by Eq. (1), the average thickness of inside portion of the tube can be found from the relation:

$$t_1 = \frac{2\pi R t_0 m h}{\left(\frac{V_{AB}}{t_1} + \frac{V_{BB'}}{t_1} + \frac{V_{B'A'}}{t_1}\right)} \tag{69}$$

2.13. Mean thickness of outside portion of fold, t_2

The circumferential radius, r, of the tube at any point which is lying in portion CA′ at a distance x from point C measured along the length of the fold is given by:

$$r = R + \rho_\alpha(\cos\alpha_3 - \cos\alpha_1) \tag{70}$$

The volume of curved portion CA′ can be calculated by integrating the elemental volume of tube from the relation:

$$V_{CA'} = 2\pi t_2 \int_0^{(1-m)h} r\,dx$$

or,

$$\frac{V_{CA'}}{t_2} = 2\pi\left[R(1-m)h + \frac{(1-\beta)^2h^2}{4\alpha^2}\sin\alpha_1 - \frac{(1-\beta)h^2(1-m)}{2\alpha}\cos\alpha_1\right] \tag{71}$$

Considering the conservation of mass i.e. equating the total volume in the deformed state to its initial volume, we get the average thickness of the tube as,

$$t_2 = \frac{2\pi R t_0 (1-m)h}{\frac{V_{CA'}}{t_2}} \tag{72}$$

where, $\frac{V_{CA'}}{t_2}$ is given by Eq. (71).

2.14. Energy absorbed in bending

The energy absorbed in bending when angle α gets incremented by $d\alpha$, is given by

$$dW_b = 2\pi\left[M_{p1}(R_A + R_B) + M_{p1}\left(1 - \frac{\alpha_1}{\alpha}\right)(R_{B'} + R_{A'}) + M_{p2}\frac{\alpha_1}{\alpha}(R_{A'} + R_C)\right]d\alpha$$

or,

$$dW_b = 2\pi k f_y \left[t_1^2\left\{2R - \frac{(1-\beta)h}{2\alpha}(2\cos\alpha_1 - 3\cos\alpha + 1) - 2\beta h\sin\alpha + \left(1 - \frac{\alpha_1}{\alpha}\right) \times \left(2R - \frac{(1-\beta)h}{2\alpha}(\cos\alpha_1 - \cos\alpha)\right)\right\} + t_2^2\frac{\alpha_1}{\alpha}\left\{2R + \frac{(1-\beta)h}{2\alpha}(1 - \cos\alpha_1)\right\}\right]d\alpha \tag{73}$$

Total bending energy can now be computed by integrating this expression from 0 to the maximum hinge angle, α_m, thus

$$W_b = 2\pi k f_y \int_0^{\alpha_m} t_1^2\left[2R - \frac{(1-\beta)h}{2\alpha}(2\cos\alpha_1 - 3\cos\alpha + 1) - 2\beta h\sin\alpha + \left(1 - \frac{\alpha_1}{\alpha}\right) \times \left\{2R - \frac{(1-\beta)h}{2\alpha}(\cos\alpha_1 - \cos\alpha)\right\}\right]d\alpha + 2\pi k f_y \int_0^{\alpha_m} t_2^2\frac{\alpha_1}{\alpha}\left(2R + \frac{(1-\beta)h}{2\alpha}(1 - \cos\alpha_1)\right)d\alpha \tag{74}$$

2.15. Circumferential energy

The circumferential energy for different portions viz. AB, BB′, B′A′ and A′C has been calculated in the following:

The change in the circumferential radius of curvature for the portion between A and B can be obtained from Eq. (63) as:

$$dr = -\frac{(1-\beta)h}{2\alpha}\left[2\sin\alpha\,d\alpha - \sin\alpha_1\,d\alpha_1 - \frac{2x}{(1-\beta)h}\sin\alpha_3\,d\alpha\right] + \frac{(1-\beta)h}{2\alpha^2}[\cos\alpha_1 - 2\cos\alpha + \cos\alpha_3]d\alpha - \beta h\cos\alpha\,d\alpha \tag{75}$$

The incremental hoop energy absorbed in the portion AB can be calculated as:

$$dW_{C1} = 2\pi t_1 f_y \int_0^{(1-\beta)h/2}\left[-\frac{(1-\beta)h}{2\alpha}\left\{2\sin\alpha\,d\alpha - \sin\alpha_1\,d\alpha_1 - \frac{2x}{(1-\beta)h}\sin\alpha_3\right\}d\alpha\,dx + \frac{(1-\beta)h}{2\alpha^2}\{\cos\alpha_1 - 2\cos\alpha + \cos\alpha_3\}d\alpha - \beta h\cos\alpha\,d\alpha\right]dx$$

or

$$\mathrm{d}W_{C1} = 2\pi t_1 f_y \frac{(1-\beta)^2 h^2}{4\alpha^2}\left[-\alpha\left\{2\sin\alpha - \frac{2(1-m)}{(1-\beta)}\sin\alpha_1\right\} - 3\cos\alpha + \cos\alpha_1 + \frac{2}{\alpha}\sin\alpha - \frac{2\beta\alpha^2}{(1-\beta)}\cos\alpha\right]\mathrm{d}\alpha \tag{76}$$

Total circumferential energy in the region AB can now be found by integrating it from $\alpha = 0$ to $\alpha = \alpha_m$.

$$W_{C1} = 2\pi f_y \frac{(1-\beta)^2 h^2}{4}\left[2\int_0^{\alpha_m} \frac{t_1 \sin\alpha}{\alpha}\left(\frac{1-\alpha^2}{\alpha^2}\right)\mathrm{d}\alpha + \frac{2(1-m)}{(1-\beta)}\int_0^{\alpha_m} \frac{t_1\sin\alpha_1}{\alpha}\mathrm{d}\alpha + \int_0^{\alpha_m} t_1 \frac{(\cos\alpha_1 - 3\cos\alpha)}{\alpha^2}\mathrm{d}\alpha - \frac{2\beta}{(1-\beta)}\int_0^{\alpha_m} t_1\cos\alpha\,\mathrm{d}\alpha\right] \tag{77}$$

The incremental circumferential energy $\mathrm{d}W_{C2}$, $\mathrm{d}W_{C3}$ and $\mathrm{d}W_{C4}$ and the corresponding total circumferential energy W_{C2}, W_{C3} and W_{C4} in the regions BB′, B′A′ and A′C respectively can similarly be found and these are given in the following:

or,

$$\mathrm{d}W_{C2} = \pi t_1 f_y \beta h^2\left[\frac{(1-\beta)}{\alpha}\left\{\frac{\cos\alpha_1 - \cos\alpha}{\alpha} - \sin\alpha\right\}\mathrm{d}\alpha + 2(1-m)\frac{\sin\alpha_1\,\mathrm{d}\alpha}{\alpha} - \beta\cos\alpha\,\mathrm{d}\alpha\right] \tag{78}$$

$$W_{C2} = \pi f_y \beta h^2\left[(1-\beta)\int_0^{\alpha_m} t_1\left\{\frac{\cos\alpha_1 - \cos\alpha - \alpha\sin\alpha}{\alpha^2}\right\}\mathrm{d}\alpha + 2(1-m)\int_0^{\alpha_m} t_1\frac{\sin\alpha_1}{\alpha}\mathrm{d}\alpha - \beta\int_0^{\alpha_m} t_1\cos\alpha\,\mathrm{d}\alpha\right] \tag{79}$$

$$\mathrm{d}W_{C3} = \pi t_1 f_y(\beta-1)h^2\left[\frac{(\beta-1)(2\sin\alpha - \alpha\cos\alpha - 2\sin\alpha_1)}{2\alpha^3}\mathrm{d}\alpha - \frac{(2m-\beta-1)(1-m)}{(\beta-1)\alpha}\sin\alpha_1\,\mathrm{d}\alpha + \frac{(3-4m+\beta)}{2\alpha^2}\cos\alpha_1\,\mathrm{d}\alpha\right] \tag{80}$$

$$W_{C3} = \pi f_y(\beta-1)h^2\left[\frac{(1-\beta)}{2}\int_0^{\alpha_m}\frac{t_1(2\sin\alpha - \alpha\cos\alpha - 2\sin\alpha_1)}{\alpha^3}\mathrm{d}\alpha - \frac{(2m-\beta-1)(1-m)}{(1-\beta)}\int_0^{\alpha_m}\frac{t_1\sin\alpha_1}{\alpha}\mathrm{d}\alpha + \frac{(3-4m+\beta)}{2}\int_0^{\alpha_m}\frac{t_1\cos\alpha_1}{\alpha^2}\mathrm{d}\alpha\right] \tag{81}$$

$$\mathrm{d}W_{C4} = \pi f_y t_2(1-\beta)h^2\left[\frac{2(1-m)^2}{(1-\beta)}\frac{\sin\alpha_1}{\alpha}\mathrm{d}\alpha + 2(1-m)\frac{\cos\alpha_1}{\alpha^2}\mathrm{d}\alpha - (1-\beta)\frac{\sin\alpha_1}{\alpha^3}\mathrm{d}\alpha\right] \tag{82}$$

$$W_{C4} = \pi f_y(1-\beta)h^2\left[\frac{2(1-m)^2}{(1-\beta)}\int_0^{\alpha_m}\frac{t_2\sin\alpha_1}{\alpha}\mathrm{d}\alpha + 2(1-m)\int_0^{\alpha_m}\frac{t_2\cos\alpha_1}{\alpha^2}\mathrm{d}\alpha - (1-\beta)\int_0^{\alpha_m}\frac{t_2\sin\alpha_1}{\alpha^3}\mathrm{d}\alpha\right] \tag{83}$$

Total incremental strain energy for the small increment in angle α by $\mathrm{d}\alpha$ for each case can be calculated as

$$\mathrm{d}W_T = \mathrm{d}W_b + 2(\mathrm{d}W_{C1} + \mathrm{d}W_{C2} + \mathrm{d}W_{C3} + \mathrm{d}W_{C4}) \tag{84}$$

Total work done for each case in crushing up to hinge angle α can then be calculated from:

$$W_\alpha = \int_0^\alpha \mathrm{d}W_\mathrm{T} = \int_0^\alpha [\mathrm{d}W_\mathrm{b} + 2(\mathrm{d}W_{\mathrm{C1}} + \mathrm{d}W_{\mathrm{C2}} + \mathrm{d}W_{\mathrm{C3}} + \mathrm{d}W_{\mathrm{C4}})] \tag{85}$$

Total energy absorbed in bending and circumferential deformation up to maximum hinge angle, α_m, can thus be calculated for each case from

$$W_\mathrm{T} = W_\mathrm{b} + 2(W_{\mathrm{C1}} + W_{\mathrm{C2}} + W_{\mathrm{C3}} + W_{\mathrm{C4}}) \tag{86}$$

3. Average crushing load

Applying the energy balance by equating the external work done to the energy absorbed in bending and circumferential deformation, the mean crushing load, P_m, can be obtained from the expression:

$$P_\mathrm{m}\delta_\mathrm{T} = W_\mathrm{T} \tag{87}$$

where, W_T is the total energy absorbed in bending and circumferential deformation to be calculated from Eq. (86) by suitably putting the values of W_b, W_{C1}, W_{C2}, W_{C3}, and W_{C4} depending upon the applicability of the case considered in the analysis above; and δ_T is the total effective crushing distance corresponding to one complete fold which is given by:

$$\delta_\mathrm{T} = 2h - t_0 - 2\rho_\mathrm{f} \tag{88}$$

where, $\rho_\mathrm{f} = \frac{(1-\beta)h}{2\alpha_\mathrm{m}}$ = final radius of curvature of curved portion of fold; and α_m is the maximum hinge angle. Eq. (87) is based on the assumption that the energy is absorbed in plastic deformation in bending and circumferential deformations only and thus neglecting the energy absorption in axial and shear deformation.

4. Size of fold and folding parameter

The size of fold, h, and the folding parameter, m, can be determined by minimizing the mean crushing load P_m, thus

$$\frac{\partial P_\mathrm{m}}{\partial h} = 0 \tag{89}$$

$$\frac{\partial P_\mathrm{m}}{\partial m} = 0 \tag{90}$$

The expression for mean crushing load being very complex, closed-form solution for h as well as m can not be found and, therefore, these can be determined numerically.

5. Variation of crushing load

The crushing load, P at any instant of crushing when the rotation of fold is α, can be calculated by

$$P = \frac{\mathrm{d}W_\alpha}{\mathrm{d}\delta} \tag{91}$$

where, W_α is the total work done in crushing up to an angle α given by the Eq. (85) and δ is the vertical compression given by:

$$\delta = 2h - 4\rho_\alpha \sin\alpha - 2\beta h\cos\alpha \tag{92}$$

and, therefore,

$$\mathrm{d}\delta = 2(1-\beta)h\frac{\sin\alpha}{\alpha^2}\mathrm{d}\alpha - 2(1-\beta)h\frac{\cos\alpha}{\alpha}\mathrm{d}\alpha + 2\beta h\sin\alpha\,\mathrm{d}\alpha \tag{93}$$

6. Mode of collapse

For the understanding of the mode of deformation, progress of collapse of round tubes for $\beta = 1/3$ as taken in (Grzebeita, 1990; Gupta and Velmurugan, 1997) has been shown in Fig. 3 The values of α for which the deformed shape of tube has been shown in these figures have been chosen arbitrarily so as to show the progress of collapse of tubes distinctly, but final value of α is the maximum hinge angle, after which no further deformation is considered in the fold. The final crushed shape of tubes for different values of β ($\beta = 0$, 1/4, 1/3, 1/2, 2/3, 3/4, 0.9 and 1) has been shown in Fig. 4. The maximum hinge angle for every case has also been mentioned under each figure. Mathematically, maximum hinge angle α_m corresponds to the stage at which crushing distance is equal to the final crushing distance δ_T given by Eq. (88). The influence of the thickness of tube on the maximum hinge angle and the mode of deformation has been neglected.

The variation of maximum hinge angle with the variation of the value of β has been plotted in Fig. 5. The variation of final radius of curvature of tube with the variation of β has also been shown in this figure. The best-fit equations for the estimation of α_m (in deg.) and final radius of curvature are given below

$$\alpha_m = -52.453\beta^3 + 139.38\beta^2 - 146.99\beta + 149.73 \tag{94}$$

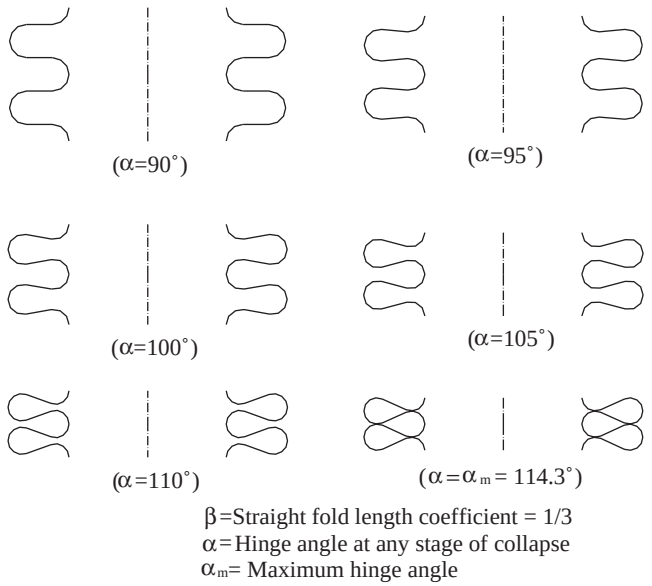

Fig. 3. Progressive collapse of round tube for $\beta = 1/3$.

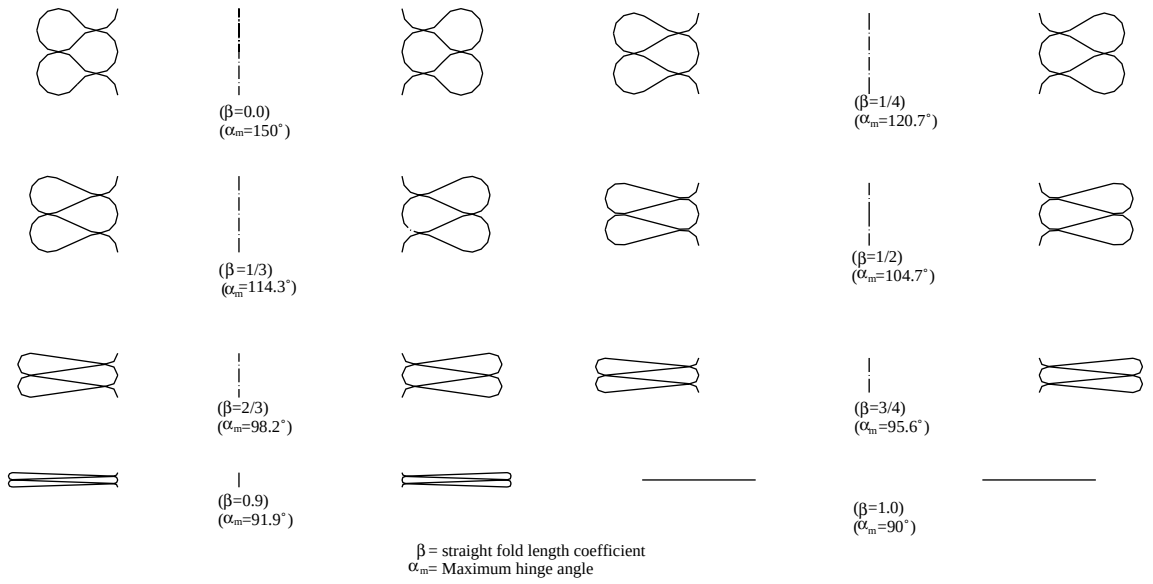

Fig. 4. Final crushed shape of round tube.

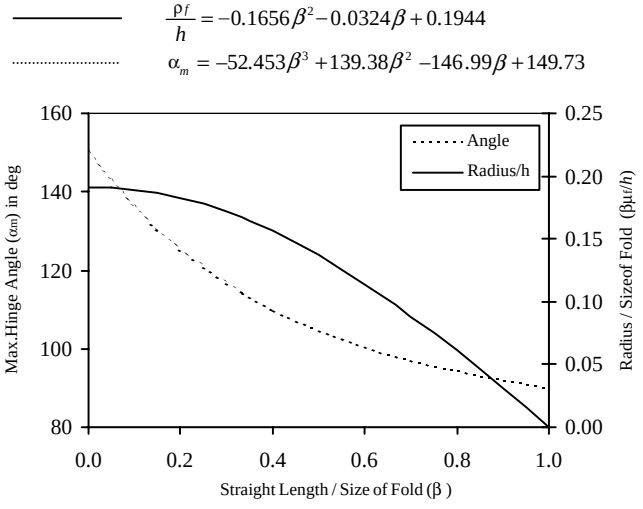

Fig. 5. Variation of hinge angle and ρ_f/h with variation in β.

and

$$\frac{\rho_f}{h} = -0.1656\beta^2 - 0.0324\beta + 0.1944 \tag{95}$$

The maximum hinge angle and the non-dimensional final radius of curvature of tube are independent of the radius of tube as well as the size of fold. The value of maximum hinge angle thus obtained for a known value of β has been used in the integration involved in the mathematical model.

7. Validation with experiments

Some experimental results involving crushing of aluminium and steel cylindrical tubes (Table 1) have been reported in literature (Gupta and Velmurugan, 1997; Gupta and Abbas, 2000, 2001). Out of these experiments, two results (Table 2) for which load–compression curves are available have been taken for the purpose of validation of the mathematical model presented in the paper.

7.1. Size of fold and folding parameter

Since no closed form solution is available for the determination of size of fold and folding parameter, these have been determined numerically by minimizing the mean crushing load using Eqs. (89) and (90). The values of size of fold and folding parameter thus calculated are reported in Tables 2–4 for outside folding, inside folding, and partly inside/outside folding respectively. The results of change in thickness of tube are also given in these tables. Four different values of β have been considered in these calculations.

It is observed from these tables that the size of fold decreases with increase in the value of β for outside folding, inside folding as well as partly inside/outside folding. The statement is true for no change in thickness as well as change in thickness also. For outside folding with increase in the value of β, the consideration of change in thickness of tube results in the increase of the size of the fold. For inside folding with increase in the value of β, the consideration of change in thickness of tube results in the decrease in the size of fold. For partly inside/outside folding with increase in the value of β, the consideration of change in thickness of tube does not have any significant effect on the size of fold.

Table 1
Experimental results involving crushing of cylindrical tubes

Parameter	Steel tube ($f_y = 400$ MPa)	Aluminium tube ($f_y = 160$ MPa)
Radius, R (mm)	21.50	24.80
Mean thickness, t_0 (mm)	1.80	1.60
Size of fold, h (mm)	17.50	6.74
Folding parameter, m	0.274	0.257
Non-dimensional mean crushing load[a], P_m/P_0	–	0.455

[a] $P_0 = 2\pi R t_0 f_y$.

Table 2
Analytical results for total outside folding[a]

Straight fold length coefficient, β	Mean crushing load, P_m/P_0	Size of fold, h (mm)	Thickness of outside portion of fold, t_2 (mm)
Steel tube			
0.0	0.615(0.496)	13.92(15.42)	1.80(1.434)
1/3	0.539(0.451)	11.96(12.96)	1.80(1.459)
2/3	0.498(0.417)	10.38(11.26)	1.80(1.462)
1.0	0.459(0.386)	09.36(10.20)	1.80(1.456)
Aluminium tube			
0.0	0.530(0.436)	13.92(15.36)	1.60(1.311)
1/3	0.469(0.399)	11.82(12.88)	1.60(1.332)
2/3	0.429(0.367)	10.36(11.20)	1.60(1.334)
1.0	0.395(0.339)	09.34(09.96)	1.60(1.333)

[a] Values within parenthesis are for change in thickness condition.

Table 3
Analytical results for total inside folding[a]

Straight fold length coefficient, β	Mean crushing load (P_m/P_0)	Size of fold h (mm)	Thickness of inside portion of fold, t_1 (mm)
Steel tube			
0.0	0.526(0.656)	13.88(12.36)	1.80(2.269)
1/3	0.478(0.580)	11.74(10.38)	1.80(2.219)
2/3	0.441(0.530)	10.26(09.26)	1.80(2.227)
1.0	0.426(0.453)	09.46(08.52)	1.80(2.239)
Aluminium tube			
0.0	0.467(0.558)	13.80(12.70)	1.60(1.961)
1/3	0.420(0.494)	11.72(10.82)	1.60(1.929)
2/3	0.385(0.452)	09.44(09.02)	1.60(1.909)
1.0	0.370(0.389)	09.44(08.62)	1.60(1.933)

[a] Values within parenthesis are for change in thickness condition.

Table 4
Analytical results for partly inside and partly outside folding

Straight fold length coefficient (β)	Mean crushing load[a] (P_m/P_0)	Folding parameter[a], m	Size of fold[a], h (mm)	Thickness of inside portion of fold, t_1 (mm)	Thickness of outside portion of fold, t_2 (mm)
Steel tube					
0.0	0.414(0.382)	0.62(0.44)	17.78(16.94)	2.116	1.538
1/3	0.392(0.373)	0.68(0.42)	14.22(14.32)	2.055	1.534
2/3	0.355(0.337)	0.52(0.46)	13.56(14.02)	2.107	1.536
1.0	0.309(0.295)	0.52(0.44)	12.82(12.90)	2.074	1.541
Aluminium tube					
0.0	0.361(0.339)	0.62(0.44)	17.90(16.50)	1.831	1.399
1/3	0.342(0.324)	0.68(0.48)	14.26(15.96)	1.856	1.392
2/3	0.307(0.293)	0.52(0.44)	13.58(13.22)	1.805	1.397
1.0	0.267(0.257)	0.52(0.46)	12.84(12.86)	1.817	1.404

[a] Values within parenthesis are for change in thickness condition.

The value of m obtained for both tubes is more than 0.5 because of lesser energy absorption in circumferential deformation for inside portion of fold (Gupta and Abbas, 2000, 2001), when change in thickness of tube is not considered.

The consideration of change in thickness is found to have reduced the value of parameter m which is due to the increase in the thickness of the inside part of fold and decrease in the thickness of the outside part of the fold, thus resisting the inside movement of the fold. The value of m for both tubes is found to range from 0.42 to 0.48. It is also observed that the value of parameter m comes closer to the experimental values after considering change in thickness for aluminium tube.

7.2. Mean crushing load

The value of non-dimensional mean crushing load 'P_m/P_0' for outside folding, inside folding and partly inside/outside folding models are given in Tables 2–4 for steel as well as aluminium tube, where $P_0 = 2\pi R t_0 f_y$ the effect of change in the thickness of tube in all the three models has also been given in these tables.

It is observed from the analysis of steel as well as aluminium tubes that the mean crushing load and hence, the total energy absorbed in crushing reduces as the value of β increases. This is true for all the three models namely outside model, inside model and partly inside/outside model.

The consideration of change in thickness in outside and partly inside/outside folding models results in decrease in mean crushing load whereas for inside folding it is vice versa. This is valid for all values of β. The influence of change in thickness on the mean crushing load is however small. The decrease in the mean crushing load in the outside fold model is due to the decrease in thickness of tube during folding whereas for inside fold model, there will be increase in thickness thus resulting in increase in mean crushing load. In the partly inside/outside fold model there will be an increase in the value of mean crushing load because of increase of thickness in the inner portion of fold and decrease in mean crushing load because of decrease in thickness in the outside portion of fold. It is due to this reason the effect of consideration of change in thickness in partly inside/outside fold model on the mean crushing load is insignificant.

In quantitative terms, the influence of change in thickness on the mean crushing load for total outside folding varies from 7% to 19% for steel tube and 14% to 17% for aluminium tube taken in the study. The corresponding values of change in mean crushing load for total inside folding vary from 6% to 24% for steel tube and 5% to 19% for aluminium tube, whereas for partly inside/outside folding the effect of change in thickness on mean crushing load is minimum and it varies from 4% to 7% for steel tube and 4% to 6% for aluminium tube. Maximum effect of change in thickness is for $\beta = 0$ (i.e. no straight length in fold) and minimum for $\beta = 1$ (i.e. total straight fold).

7.3. Load–deformation curves

The size of fold and the folding parameter determined numerically by minimizing the mean crushing load have been used for finding out the variation of crushing load.

The load–deformation curves for all the three models (i.e. outside, inside and partly inside/outside models) for different values of β and for constant as well as varying thickness have been shown in Figs. 6–11 for steel tube (b in the legend of figures may be read as β). The analytical load–deformation curves are not starting from zero load level due to the neglect of the elastic deformation in the beginning. For all the three models with constant as well as varying thickness of tube, the reduction in value of β brings the analytical load–deformation curves closer to the experimental curves.

With change in thickness in outside and partly inside/outside folding models, the load–deformation curve drifts away from the experimental curve, whereas for inside folding it is vice versa. This holds for all values of β.

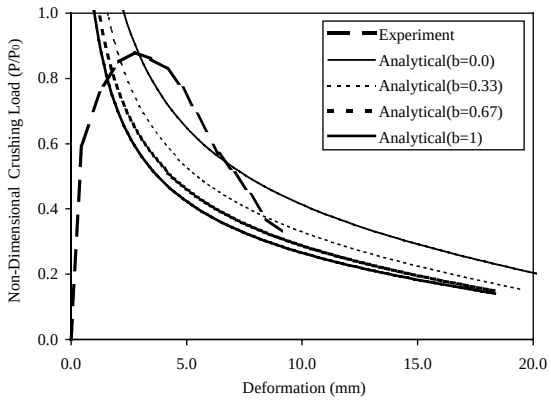

Fig. 6. Load compression curves of $R = 21.5$ mm, $t_0 = 1.8$ mm steel tube for outside folding with no change in thickness.

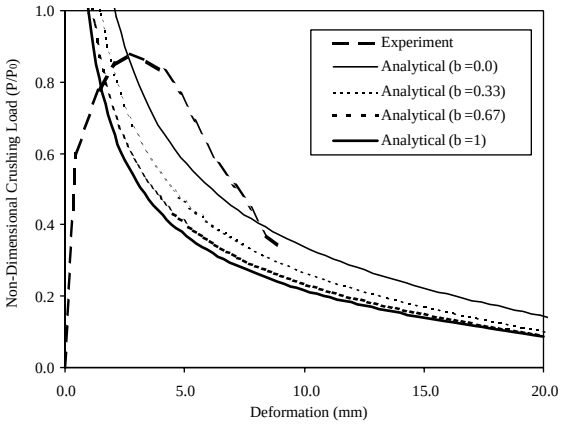

Fig. 7. Load compression curves of $R = 21.5$ mm, $t_0 = 1.8$ mm steel tube for outside folding with change in thickness.

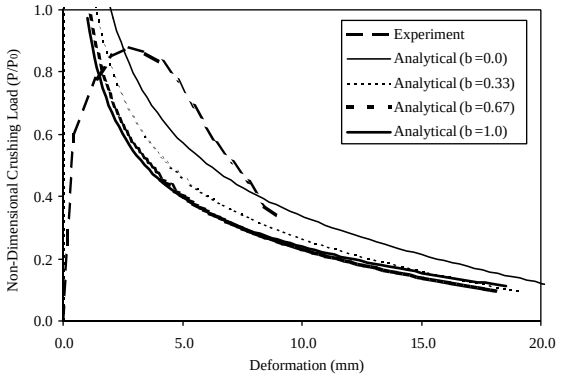

Fig. 8. Load compression curves of $R = 21.5$ mm, $t_0 = 1.8$ mm steel tube for inside folding with no change in thickness.

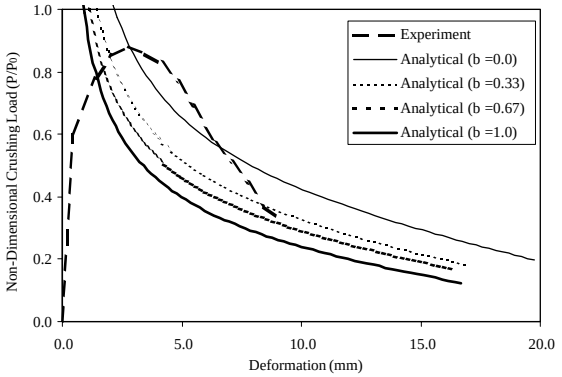

Fig. 9. Load compression curves of $R = 21.5$ mm, $t_0 = 1.8$ mm steel tube for inside folding with change in thickness.

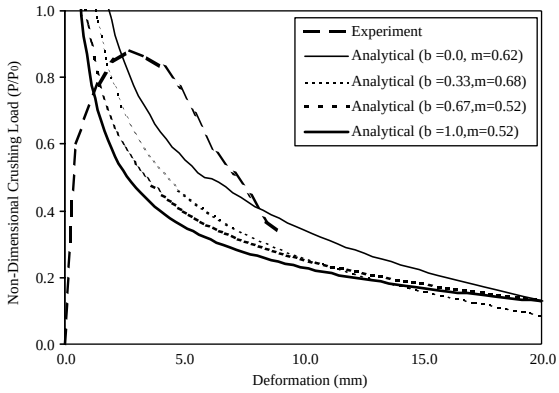

Fig. 10. Load compression curves of $R = 21.5$ mm, $t_0 = 1.8$ mm steel tube for partly inside and partly outside folding with no change in thickness.

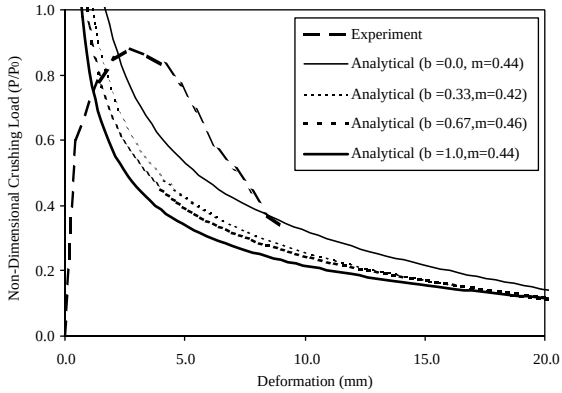

Fig. 11. Load compression curves of $R = 21.5$ mm, $t_0 = 1.8$ mm steel tube for partly inside and partly outside folding with change in thickness.

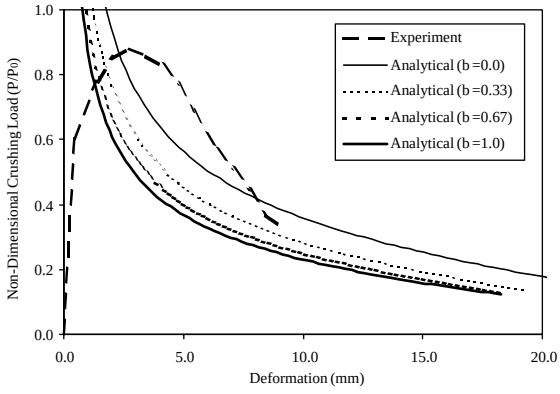

Fig. 12. Load compression curves of $R = 24.8$ mm, $t_0 = 1.6$ mm aluminium tube for outside folding with no change in thickness.

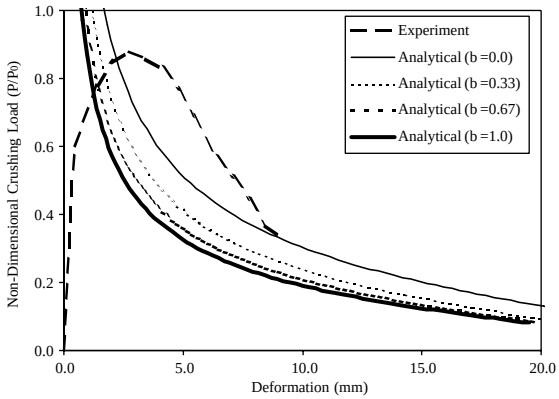

Fig. 13. Load compression curves of $R = 24.8$ mm, $t_0 = 1.6$ mm aluminium tube for outside folding with change in thickness.

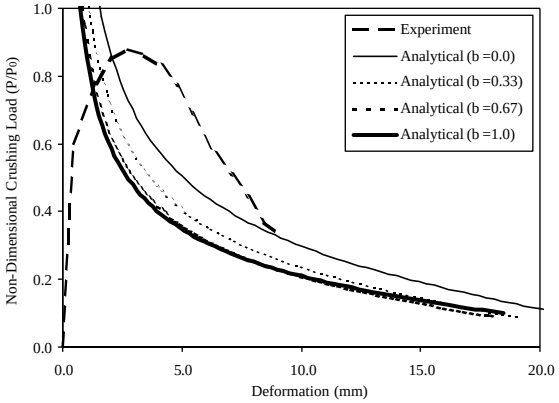

Fig. 14. Load compression curves of $R = 24.8$ mm, $t_0 = 1.6$ mm aluminium tube for inside folding with no change in thickness.

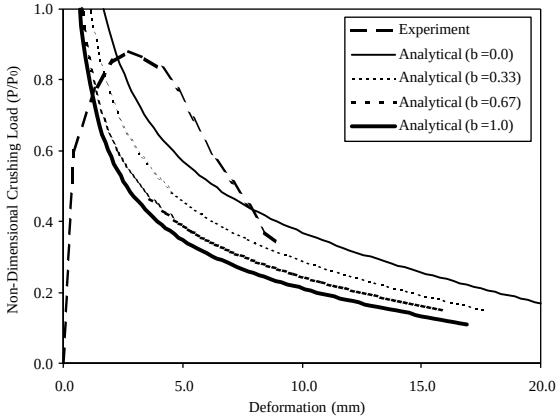

Fig. 15. Load compression curves of $R = 24.8$ mm, $t_0 = 1.6$ mm aluminium tube for inside folding with change in thickness.

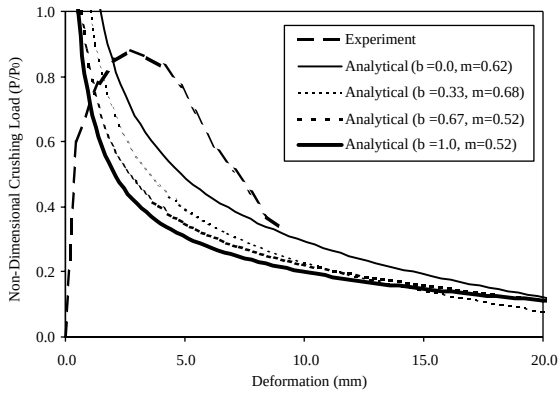

Fig. 16. Load compression curves of $R = 24.8$ mm, $t_0 = 1.6$ mm aluminium tube for partly inside and partly outside folding with no change in thickness.

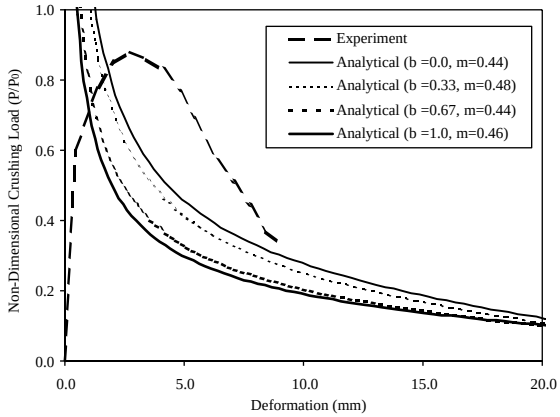

Fig. 17. Load compression curves of $R = 24.8$ mm, $t_0 = 1.6$ mm aluminium tube for partly inside and partly outside folding with change in thickness.

For aluminium tube, similar observations are made. The results have been plotted in Figs. 12–17 (b in the legend of figures may be read as β).

8. Conclusions

In the present paper, a curved fold model with variable straight length and variation in the thickness of tube has been developed. The variation of circumferential strain during the formation of fold has been taken into consideration. The present model considers partly inside and partly outside folds and thus total outside and total inside fold models can be easily derived. Optimal value of folding parameter, m, has been evaluated analytically. An expression has been derived for determining the variation of crushing load during fold formation. The maximum hinge angle and the final radius of curvature of fold have been determined mathematically.

The size of fold decreases with increase in the value of β for outside folding, inside folding as well as partly inside and partly outside folding with no change in thickness. The consideration of change in thickness in the partly inside and partly outside folding does not have any significant effect on the size of fold. For outside folding and for known value of β, the consideration of change in thickness of tube results in the increase in the size of fold, and vice versa in the case of inside folding. The folding parameter, m, reduces when change in the thickness of tube during the formation of fold is incorporated in the model thus bringing it closer to the experiments. The mean crushing load reduces with increase in the value of β. The results have been compared with experiments.

References

Abbas, H., Paul, D.K., Godbole, P.N., Nayak, G.C., 1989. Mathematical modeling of soft missile impact on protective walls. In: Proceedings of International Conference on Software Application in Engineering, IIT Delhi, pp. 577–581.

Abbas, H., Paul, D.K., Godbole, P.N., Nayak, G.C., 1995. Soft missile impact on rigid targets. International Journal of Impact Engineering 16 (5), 727–737.

Abbas, H., Tyagi, B.L., Arif, M., Gupta, N.K., 2003. Curved fold model analysis for axi-symmetric axial crushing of tubes. Thin Walled Structures 41, 639–661.

Abramowicz, W., Jones, N., 1984. Dynamic axial crushing of circular tubes. International Journal of Impact Engineering 2, 263–281.

Alexander, J.M., 1960. An approximate analysis of the collapse of thin cylindrical shells under axial loading. Quarterly Journal of Mechanics and Applied Mathematics 13, 10–15.

Grzebeita, R.H., 1990. An alternative method for determining the behaviour of round stocky tubes subjected to an axial crushing load. Thin Walled Structures 9, 61–89.

Gupta, N.K, Abbas, H., 2000. Mathematical modeling of axial crushing of cylindrical tubes. Thin Walled Structures 38, 355–375.

Gupta, N.K., Abbas, H., 2001. Some considerations in axi-symmetric folding of metallic round tubes. International Journal of Impact Engineering 25, 331–344.

Gupta, N.K., Gupta, S.K., 1993. Effect of annealing, size and cut-outs on axial collapse behaviour of circular tubes. International Journal of Mechanical Science 35, 597–613.

Gupta, N.K., Velmurugan, R., 1997. Consideration of internal folding and non-symmetric fold formation in axi-symmetric axial collapse of round tubes. International Journal of Solids and Structures 34 (20), 2611–2630.

Mamalis, A.G., Johnson, W., 1983. The quasi-static crumpling of thin-walled circular cylinders and frusta under axial compression. International Journal of Mechanical Science 25, 713–732.

Wierzbicki, T., Bhat, S.U., Abramowicz, W., Brodkin, D., 1992. Alexander revisited—a two folding elements model of progressive crushing of tubes. International Journal of Solids and Structures 29 (24), 3269–3288.